Role of an N-Terminal Loop in the Secondary Structural Change of Photoactive Yellow Protein†

Miki Harigai, Yasushi Imamoto,* Hironari Kamikubo, Yoichi Yamazaki, and Mikio Kataoka

Graduate School of Materials Science, Nara Institute of Science and Technology, Ikoma, Nara 630-0192, Japan

Received May 16, 2003; Revised Manuscript Received September 5, 2003

ABSTRACT: Photoactive yellow protein (PYP) is photoconverted to its putative active form (PYP_M) with global conformational change(s). The changes in the secondary structure were studied by far-UV circular dichroism (CD) and Fourier transform infrared (FTIR) spectroscopy using PYP, which lacks N-terminal 6, 15, or 23 amino acid residues (T6, T15, and T23, respectively). Irradiation of truncated PYPs induced the loss of the CD signal, where the maximal difference was located at 222 nm. The reduction of the CD signal was significantly larger than the calculated CD of the N-terminal helices, indicating that it is mainly accounted for by the unfolding and/or structural change of the helices located outside the N-terminal region. The difference FTIR spectra between dark and photosteady states recorded using the solution samples demonstrated that large absorbance changes in the amide mode of the β-sheet were reduced and downshifted by truncation. The structural change of the β-sheet is therefore closely correlated with the N-terminal loop. NaCl decelerates the decay of intact PYP_M and $T6_M$ at low concentrations ($<$500 mM) but accelerates decay at high concentrations ($>$1000 mM). For $T15_M$ and $T23_M$, NaCl accelerates their decay at $>$100 mM but never decelerates their decay, suggesting that the electrostatic interaction, which plays an important role for the recovery of PYP from PYP_M, is lost by removing positions 7−15. The electrostatic interaction between this region and the β-scaffold is likely to promote the conformational change of PYP_M for recovery of PYP.

Since the interconversion between the inactive form and the active form of the receptor protein is driven by a global conformational change induced by the stimulus, study of the structural change is essential in elucidating the transduction mechanism for receptor proteins. Photoreceptor proteins are widely subjected to this kind of study, and photoactive yellow protein (PYP)[1] is one of the most-characterized photoreceptor proteins.

PYP is a soluble photoreceptor protein found in the purple phototropic bacterium *Ectothiorhodospira halophila* (*1*). It consists of four segments called an N-terminal cap (containing α1 and α2 helices), a PAS core (strands β1, β2, α3, α4, and β3), a helical connector (α5), and a β-scaffold (β4, β5, and β6) (*2*). On the basis of its sequential homology, PYP is thought to be a prototype of the PAS domain superfamily, which is widely involved in the signal transduction system. PYP has been proposed to be the photoreceptor for photophobic reactions in bacteria (*3*). For photon absorption, PYP undergoes a photocycle, in which several spectroscopically distinct intermediates are formed (*4*−*8*). The lifetimes as well as the spectral shifts of PYP intermediates are similar to those of bacterial retinal proteins, such as sensory rhodopsin (*9*, *10*) and phoborhodopsin (sensory rhodopsin II) (*11*), while the chromophore of PYP is a *p*-coumaric acid bound to a cysteine residue by a thioester bond. Despite the strikingly different properties of the protein moiety and chromophore, the long-lived intermediate, PYP_M (also called pB or I2), is thought to correspond to M (meta) intermediates of bacterial retinal proteins in a spectroscopic analogy. They have the following common features: (i) they are relatively stable intermediates in their photocycle, with lifetimes of 0.1−1 s. (ii) Their chromophores are electronically neutral, while in dark states they are charged (positive for retinal proteins and negative for PYP). (iii) Their absorption spectra are located in the near-UV region. (iv) They have chromophores in cis forms, unlike their dark states.

The transducer has not been identified in the PYP system, but PYP_M is thought to be the active form. Structural analysis of PYP_M is thus essential to revealing the activation mechanism for PYP. The tertiary structure of PYP_M was first proposed by time-resolved crystallography (*12*). This model proposed that the chromophore and nearby amino acid side chains are rearranged in PYP_M, and the positive charge of Arg52 is exposed. This change of the surface charge distribution was confirmed in solution by probing the surface of PYP_M using multivalent organic acids such as citrate (*13*). Since then, the mechanism for formation of PYP_M has been studied extensively, and a lot of spectroscopic data has been accumulated. It has been shown that PYP_M is formed by

† This work was supported in part by a Grant-in-Aid for Scientific Research from the Ministry of Education, Culture, Sports, Science and Technology of Japan and by a grant from Sekisui Integrated Research Inc.

* To whom correspondence should be addressed. Phone: +81-743-72-6101. Fax: +81-743-72-6109. E-mail: imamoto@ms.aist-nara.ac.jp.

[1] Abbreviations: PYP, photoactive yellow protein from *Ectothiorhodospira halophila*; PAS, per-arnt-sim; SAXS, small-angle X-ray scattering; R_g, radius of gyration; FTIR, Fourier transform infrared; CD, circular dichroism; MOPS, 3-(*N*-morpholino)propanesulfonic acid; *i*PYP, intact PYP; T*n*, PYP in which N-terminal *n* amino acid residues were truncated.

10.1021/bi034814e CCC: $25.00
Published on Web 11/05/2003

proton transfer from Glu46 to the phenolic oxygen of the chromophore (*14*, *15*), followed by a global conformational change in the protein moiety (*16*−*19*). The protein conformational change is so large that PYP_M is in a partially denatured state (*20*−*22*). These findings clearly show that the structural change in solution is significantly larger than that in the crystal (*18*); therefore, analysis of PYP_M under physiological conditions is required.

Our recent SAXS experiments have demonstrated that the R_g of PYP_M is 0.4−1.1 Å larger than that of PYP (15.2 Å) (*13*, *23*). This dimensional increase is reduced, and the lifetime of PYP_M is markedly prolonged when several N-terminal amino acid residues are cleaved (*23*−*25*), suggesting that the N-terminal region has crucial roles in the conformational changes for the formation and decay of PYP_M. However, FTIR studies in solution demonstrated that a large absorbance change in the amide I region is observed in the PYP_M/PYP spectrum, and it is partially attributable to the antiparallel β-structure (*18*). These observations suggest that the β-sheet and N-terminal region are involved together in the conformational change. The next question is what interactions are present between the β-sheet and the N-terminal region and how they are rearranged in PYP_M. In the present study, the role of the N-terminal region for the changes in secondary structure was studied by CD and FTIR spectroscopy, using PYPs with enzymatically truncated N-terminal regions (6−23 amino acid residues). In addition, the effect of the salt concentration on the decay of PYP_M was studied to examine what kind of interaction promotes the decay of PYP_M.

MATERIALS AND METHODS

Sample Preparation. Intact PYP (*i*PYP) was prepared using a heterologous overexpression system in *Escherichia coli* (*26*, *27*). Truncated PYPs, which lack N-terminal 6, 15, and 23 residues (T6, T15, and T23, respectively), were prepared by partial digestion with chymotrypsin followed by isolation using DEAE-Sepharose column chromatography (*24*).

CD Spectroscopy. CD spectra were measured with a J-725 circular dichroism spectropolarimeter (Jasco, Tokyo, Japan). The sample (~1 μM protein, 10 mM MOPS, 200 mM NaCl, pH 7.0) was put into a quartz cell with a 1 cm light path length. The temperature of the sample was kept at 283 K with a Peltier temperature controller (PYC-347WI; Jasco, Tokyo, Japan). CD spectra for M intermediates were measured under continuous illumination with yellow light (>410 nm) obtained using a 100-W optical fiber illuminator (Megalight 100, Hoya-Schott, Tokyo, Japan) and a glass optical filter (Y43, Asahi Techno Glass, Chiba, Japan). As the penetration of actinic light into the detector causes an inaccuracy in the CD signal, it was protected with a band-pass filter (maximum transmittance = 220 nm, fwhm = 40 nm) (BP-0220-040-A; Spectrogon, Täby, Sweden). The voltage of the photomultiplier was not fluctuated by illuminating the sample, indicating that the actinic light is practically blocked by this filter.

As the control experiments, CD spectra of E46Q (pH 8.0) were measured in the dark without the band-pass filter, in the dark with the filter, and under illumination with the filter. Because the lifetime of $E46Q_M$ is much shorter than that of *i*PYP_M, no $E46Q_M$ was accumulated in our experimental conditions. These CD spectra were identical, indicating that no spectral artifact was produced by the filter or the actinic light.

The CD produced by each α-helix and β-sheet of PYP was calculated on the basis of its crystal structure (PDB entry 2PHY). The molar ellipticity of α-helix of n peptide units at 222 nm is empirically represented as follows (*28*):

$$[\theta]_{222} = CD_{max}(1 - k/n)$$

Where CD_{max} and k are the molar ellipticity of the α-helix of infinite length and the empilical constant, respectively. However, it was recently reported that the ellipticity of the short helix does not obey this rule (*29*). The values of k vary according to the length of helix: $k = 2.8$ for $n = 4$, $k = 3.5$ for $n = 8$, and $k = 4.0$ for $n = 11$ (thus k for $n = 7$ is deduced to be 3.3). In the present analysis, the value of 2.8 was used for α1, α2, and α4; 3.3 for α3; and 4.0 for α5. CD_{max} was estimated to be −43 000 (*29*).

The ellipticity of the random coil was neglected because the ellipticity of PYP denatured by 9 M urea at 222 nm was less than 3% of the native PYP (data not shown). The molar ellipticity of the β-strands was estimated to be −15 000 by the k2d program (*30*).

FTIR Spectroscopy. FTIR spectra were recorded using a BioRad FTS-6000 Fourier transform infrared spectrophotometer. The temperature of the sample was maintained at 293 K by an Oxford Optistat DN optical cryostat (Witney, Oxfordshire, UK). The sample cell was composed of two CaF_2 windows (18 mm diameter) and a Capton film spacer (7.2 μm thickness; Dupont-Toray, Tokyo, Japan), in which 5 μL of the sample (~160 mg/mL protein, 10 mM MOPS, 200 mM NaCl, pH 7.0) was placed. The sample cell was set at an angle of 45° and irradiated perpendicularly to the monitoring beam for excitation. The irradiation light at 436 nm (fwhm = 10 nm) was obtained by an optical interference filter (43161; Edmund Scientific, Barrington, NJ) and a 150 W cold light source (HL150; Hoya-Schott, Tokyo, Japan).

UV−*Vis Absorption Spectroscopy.* The decay of *i*PYP_M, $T6_M$, $T15_M$, and $T23_M$ in 10 mM MOPS buffer (pH 7.0) was monitored by the absorbance change at 350 nm after photoexcitation at 293 K. *i*PYP and T6 were excited by >410-nm light, obtained by a short-arc xenon flash lamp (SA200; Eagle, Kanagawa, Japan) with a glass optical filter (Y43; Asahi Techno Glass, Chiba, Japan). The absorbance changes were recorded with a multichannel CCD/fiber optic spectroscopy system (S2000 system; Ocean Optics, Dunedin, FL). As the lifetimes of $T15_M$ and $T23_M$ are extremely long (2−20 min), the absorbance changes for $T15_M$ and $T23_M$ were precisely measured using a Shimadzu UV2400PC double-beam spectrophotometer (Kyoto, Japan). T15 and T23 were excited by illumination for 2 s using a 60-W cold light fiber optical illumination system (Luminar Ace LA-60Me, Hayashi Watch-Works, Osaka, Japan) and a glass optical filter (Y43, Asahi Techno Glass). The absorbance decrease was fitted by a single-exponential function by IGOR Pro version 3.1 (WaveMetrics, Lake Oswego, OR) to estimate decay rate constants.

RESULTS

CD Spectroscopy. PYP has two short α-helices in the N-terminal cap (α1 and α2), two in the PAS core (α3 and

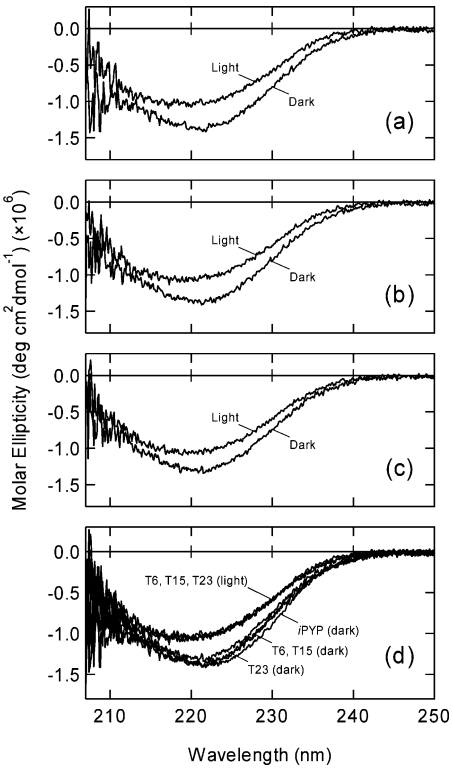

FIGURE 1: Far-UV CD spectra of truncated PYPs and their M intermediates. CD spectra of T6 (a), T15 (b), and T23 (c) were measured in the dark and under continuous illumination with yellow light (>410 nm) at 283 K. Ellipticity was converted to molar ellipticity per protein. (d) CD spectra of *i*PYP, T6, T15, T23, $T6_M$, $T15_M$, and $T23_M$ as compared to each other.

α4), and one in the helical connector (α5) (*2*). All α-helices are conserved in T6, T15 lacks α1, and T23 lacks α1 and α2. The α-helices and the *β*-sheet produce the negative CD signal at 222 nm. It has been reported that the intensity of the CD signal is reduced upon the formation of PYP_M (*21*, *22*). This is explained by the partial loss of secondary structure, but site-specific information has not been reported. The far-UV CD spectra of *i*PYP, T6, T15, and T23 were measured in the dark (Figure 1). Then spectra for $T6_M$, $T15_M$, and $T23_M$ were measured under continuous illumination with >410 nm light (Figure 1). The CD signals were converted to molar ellipticity per protein. Under these experimental conditions, 14% of *i*PYP was converted to *i*PYP_M, whereas >90% of T6, T15, and T23 was converted to their respective M intermediates (data not shown). As the reduction of CD at 222 nm was 3.8% for *i*PYP in this condition (data not shown), the molar ellipticity of *i*PYP_M at 222 nm was calculated to be -1.00×10^6 deg cm^2 dmol^{-1}. The ellipticities at 222 nm are presented in Figure 2. The fractions of secondary structures could not be estimated solely from the ellipticity at 222 nm, but ellipticity can be accurately estimated from the protein structure. To speculate the composition of the CD signal of *i*PYP, the CD signal produced by each α-helix and *β*-sheet derived from the crystal structure was calculated (see Materials and Methods). It is also presented in Figure 2 for comparison.

The far-UV CD signal in the dark was only slightly reduced by truncation because α1 and α2 have a small ellipticity at 222 nm due to their shortness. The calculated ellipticity of *i*PYP is significantly smaller than that experimentally obtained. A short *π*-helix (Asn61-Ala67) might account for this difference (see Discussion).

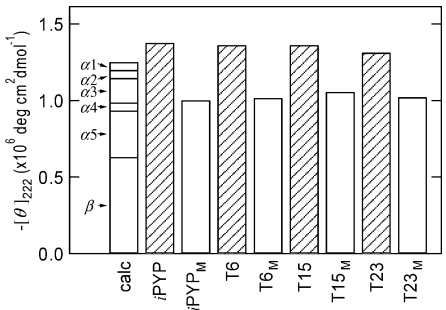

FIGURE 2: Molar ellipticity at 222 nm for the dark states (hatched bars) and M intermediates (open bars). The ellipticity of dark state *i*PYP calculated on the basis of the crystal structure (PDB entry 2PHY) is shown for comparison.

The irradiation caused a blue-shift of the CD peak along with a reduction in intensity by 27% for *i*PYP, 25% for T6 and T15, and 21% for T23. The molar ellipticities of *i*PYP_M, $T6_M$, $T15_M$, and $T23_M$ were identical, indicating that the contribution of the N-terminal loop to far-UV CD spectra was negligible. Maximal difference between dark and light conditions was located at 222 nm, which agrees with the CD peak of an α-helix (222 nm) but is different from that of a *β*-sheet (217 nm). Hence, the difference in the CD signal by illumination is mainly attributable to the α-helices, although the *β*-sheet may have a small contribution. The large decrease of CD suggests that the significant portion of α3 and/or α5 (and possibly a *π*-helix and/or *β*-sheet) would undergo the unfolding and/or structural change (Figure 2).

FTIR Spectroscopy. The absorbance change of the amide I mode in the difference FTIR spectrum between PYP_M and PYP (PYP_M/PYP spectrum) shows a protein structural change upon PYP → PYP_M conversion (*17*, *18*). However, the intensity of this mode in the crystal or frozen sample is much weaker than that in solution (*14*, *18*, *31*), indicating that the crystallization or freezing of the sample inhibits the protein structural change of PYP. Therefore, the solution sample (∼160 mg/mL) was used in the present FTIR experiments.

The FTIR spectra of T6, T15, or T23 in the dark and in the photosteady state mixture produced by 436 nm light were measured (pH 7.0, 293 K). Then the difference FTIR spectra of $T6_M$/T6, $T15_M$/T15, and $T23_M$/T23 were calculated by subtraction (positive signals for intermediates, negative signals for dark states) (Figure 3). As the control, the *i*PYP_M/*i*PYP spectrum was also measured, which was in good agreement with that recorded by the time-resolved measurement (*17*).

First, the *i*PYP_M/*i*PYP spectrum measured at 293 K was compared with that at 233 K (*14*, *31*). Both had a cis/trans marker of the chromophore at 1286/1301 cm^{-1} (*31*), confirming that both M intermediates have a cis chromophore. A protonated Glu46 band at 1737 (−) cm^{-1}; deprotonated-chromophore bands at 1437 (−), 1301 (−), and 1163 (−) cm^{-1}; and other chromophore bands at 1058 (−), 1042 (−), and 984 (−) cm^{-1} were also observed in the frozen sample. However, the intensities of the bands at 1696 (−), 1646 (−), 1530 (−), 1673 (+), 1625 (+), 1608 (+), and 1574 (+) cm^{-1} in solution were markedly larger than that in the frozen sample. On the other hand, the bands at 1487 (−), 1193 (+), and 1004 (+) cm^{-1} were located at 1482, 1177, and 994

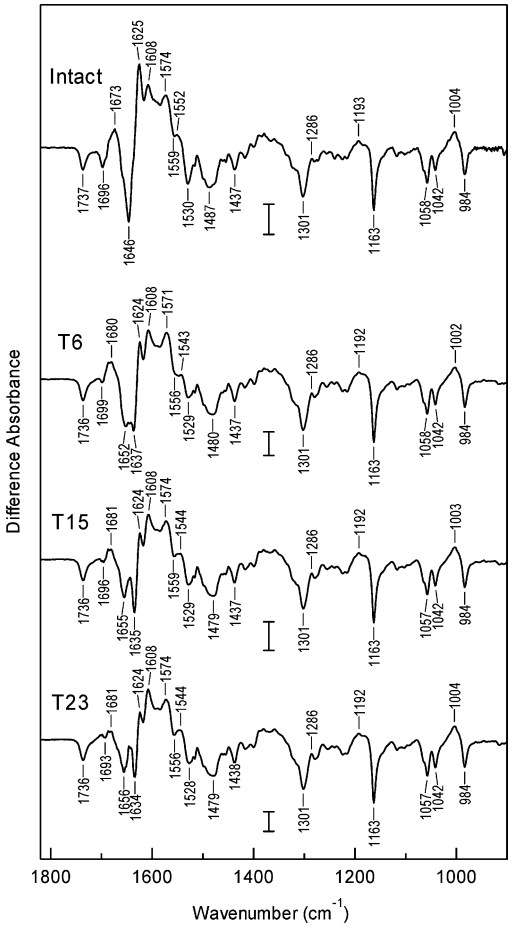

FIGURE 3: Difference FTIR spectra of *i*PYP$_M$/*i*PYP, T6$_M$/T6, T15$_M$/T15, and T23$_M$/T23. Calculated by subtracting FTIR spectra in the dark from those under continuous illumination with 436 nm light. Temperature of the measurements was 293 K. Scale bars represent 0.0002 for *i*PYP and 0.005 for T6, T15, and T23.

cm^{-1} in the frozen sample, respectively. Most of the chromophore bands in the dark state were not affected by freezing, but the chromophore bands of PYP$_M$ and the amide mode band were shifted or reduced. This can be explained by the difference between the structures of PYP$_M$ in solution and in the frozen sample.

By truncation, the intensities as well as the locations of negative bands at 1736, 1437, 1301, 1163, 1058, 1042, and 984 cm^{-1}, ascribed to Glu46 or chromophore, were not shifted, suggesting that the chromophore structure was not affected by truncation. However, the intensities of the amide mode bands were reduced as the number of truncated amino acid residues increased.

An expanded view of the amide mode region is shown in Figure 4a. The amide I mode at 1625/1646 cm^{-1} of the *i*PYP$_M$/*i*PYP spectrum was slightly downshifted, and the intensity was reduced in the T6$_M$/T6 spectrum. The intensity and wavenumber of the 1625 (+) cm^{-1} band of T6$_M$ was comparable to those of T15$_M$ and T23$_M$. However, the 1646 (−) cm^{-1} band for *i*PYP was completely separated into two bands in T15 and T23. The bands at 1697 (−) and 1530 (−) cm^{-1} were reduced in truncated PYPs. The 1673 (+) cm^{-1} band of *i*PYP$_M$ was 7 cm^{-1} upshifted in T6$_M$ and reduced in T15$_M$ and T23$_M$.

To separate several bands, which may overlap in this region, second derivative spectra are shown (Figure 4b). The

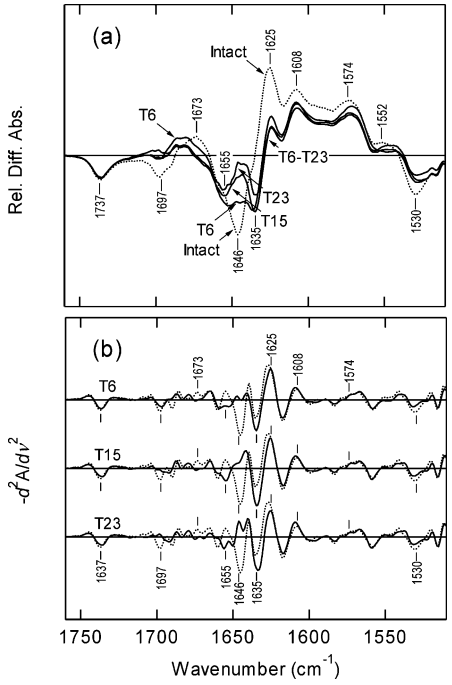

FIGURE 4: Difference FTIR spectra (a) and the second derivative spectra (b) in the amide mode region. Intensity was normalized by 1163 cm^{-1} bands. The *i*PYP$_M$/*i*PYP spectra are represented with dotted lines. Note that $-d^2A/d\nu^2$ was plotted in panel b so that the directions of the peaks in panels a and b are identical.

prominent 1625/1646 cm^{-1} band in *i*PYP$_M$/PYP is composed of a positive band at 1625 cm^{-1} and two negative bands at 1646 and 1635 cm^{-1}. It is clear that the 1646 (−) cm^{-1} band of *i*PYP disappeared in truncated PYPs. Instead, the 1655 (−) and 1635 (−) cm^{-1} bands are intensified, suggesting that the 1646 cm^{-1} band of *i*PYP is the sum of two bands, each of which shifted to 1655 or 1635 cm^{-1} by truncation. These values agree with the typical amide I modes for the α-helix and antiparallel *β*-sheet (1653 and 1632 cm^{-1}, respectively (*32*, *33*)). As the 1625 cm^{-1} band of *i*PYP$_M$ has previously been assigned to the amide I mode of the antiparallel *β*-structure (*18*), pairs of bands at 1625/1635 and 1625/1646 cm^{-1} of *i*PYP would demonstrate a structural change of the *β*-sheet. The 1673 cm^{-1} band of *i*PYP, which was upshifted in truncated PYPs, would be complementary to the 1646 (1655) cm^{-1} band. An upshift suggests structural disorder of the α-helices of PYP$_M$. The wavenumber of the 1530 cm^{-1} band for *i*PYP agrees with that of the amide II mode of the *β*-sheet (*33*). The 1697 cm^{-1} band has been assigned to an NH group of the side chain (*18*).

Effect of Salt on the Recovery of PYP. To examine for what kind of interaction the N-terminal region is responsible, the effect of salt concentration on the recovery of truncated PYPs from their M intermediates was studied. *i*PYP, T6, T15, and T23 were excited by light, and the decays of their M intermediates were monitored by an absorbance decrease at 350 nm. The decay curves were fitted by single-exponential functions, and decay rate constants were estimated. They were plotted against the NaCl concentration in the sample (Figure 5).

The rate constants were reduced as the number of truncated amino acid residues increased, as reported previously (*24*). In addition, NaCl dependence of the decays of *i*PYP$_M$ and T6$_M$ were different from that of T15$_M$ and T23$_M$. NaCl

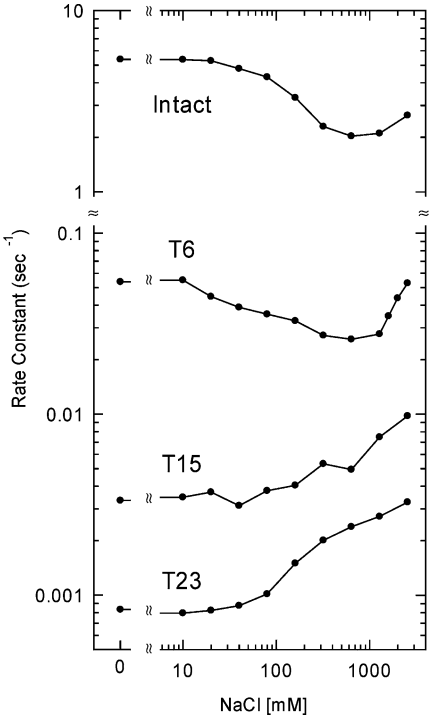

FIGURE 5: Effect of salt concentration on the decay rate constant of M intermediates. The decay rate constants were estimated by fitting the absorbance change at 350 nm in 10 mM MOPS buffer (pH 7.0, 293 K) with single-exponential functions. Decay rates are plotted against the concentration of NaCl.

decelerates the decay of iPYP$_M$ and T6$_M$ at <500 mM but accelerates decay at >1 M. The minima of decay rate constants were located at ~600 mM NaCl, where they were 2−3 times smaller than those at 0 mM NaCl. However, salt dependent deceleration was not observed for T15$_M$ and T23$_M$. Their decays were accelerated at NaCl concentrations of >100 mM, and their rate constants at 3 M NaCl were ~4 times greater than those at 0 mM. It should be noted that the effect of truncation was prominent at low salt concentrations: at <50 mM NaCl, decays of T6$_M$, T15$_M$, and T23$_M$ were 100, 2000, and 6000 times slower than iPYP$_M$, respectively, while at 3 M, they were 50, 300, and 800 times slower.

DISCUSSION

To characterize PYP$_M$ in detail, we have developed methods to stabilize PYP$_M$ by truncating N-terminal amino acid residues. In these kinds of experiments, the nature of PYP$_M$ that is altered by stabilization should be noted. We have reported that the absorption spectrum of PYP and PYP$_M$ is not largely affected by truncation (*24*). SAXS experiments have shown that the R_g values of T6, T15, and T23 in solution agree with those calculated from the crystal structure of iPYP (PDB entry 2PHY), in which atoms for N-terminal 6, 15, and 23 amino acid residues were deleted (*23*). These observations show that the disorder of protein structure by truncation is within the detection limit of SAXS experiments (*23*), and the chromophore/protein interaction is conserved in truncated PYPs.

In the present study, the secondary structural change upon the PYP → PYP$_M$ transition was examined by CD and FTIR using truncated PYPs. The far-UV CD signal was only slightly reduced by truncation in the dark but significantly reduced by light. Nowadays, the fractions of secondary structures are widely estimated by fitting the CD spectra over a broad wavelength range. It is useful to predict the secondary structure of unknown protein, but it does not perfectly reproduce the secondary structure of PYP at present. For example, the CDsstr program gave the values of 24% for the α-helix and 20% for the β-sheet (*34*). However, fractions of α-helices and β-sheets in the crystal structure are 28 and 34%, respectively. We also analyzed our CD data using the programs available now, but the similar tendency was observed (not shown).

On the other hand, the relation between ellipticity at 222 nm and secondary structure is well-investigated (*35*), and the ellipticity can be accurately estimated from the tertiary structure. In the present study, the CD at 222 nm produced by each α-helix and β-sheet was calculated using up-to-date parameters (*29*) and compared with the experimental data (Figure 2).

The molar ellipticity of iPYP was significantly larger than that calculated on the basis of the crystal structure. PYP has a short π-helix composed of seven amino acid residues (Asn61-Ala67) close to the chromophore-binding site (Cys69). A π-helix is a rare secondary structure, but its significance for function has been proposed (*36*). The CD spectrum of a π-helix has not been characterized, but the molar ellipticity of iPYP is consistent with the calculated one, on the assumption that the CD spectrum of a π-helix is comparable to that of an α-helix.

Illumination reduced the CD signal at 222 nm by 21−27%. The maximal difference was located at 222 nm, which agrees with the CD peak of an α-helix (222 nm) but is different from that of a β-sheet (217 nm). Hence, the difference in the CD signal is mainly attributable to the α-helices. In fact, it was reported that the change in CD of the β-sheet upon acidification of PYP, which mimics the PYP → PYP$_M$ transition, is much smaller than that of α-helix (*34*). NMR study proposes the structural change of the chromophore-containing loop as well as α3, α4, and the first turn of α5 (*19*), suggesting that the CD signal from these helices and/or the π-helix would be reduced. The simplest explanation for the loss of the CD signal is the (partial) unfold. Shortening of the helix simultaneously reduces the molar ellipticity of the rest of the α-helix (*28*). In addition, changes in dihedral angles also alter the CD signal (*35*).

The light-induced reduction of ellipticity at 222 nm has been investigated previously. When a high accumulation of the M intermediate was achieved by acidification of the wild type (pH 4.0) (*21*) or use of the M100L mutant (*22*), the loss of CD was 19 and 40%, respectively. The present experiment showed a 27% loss for iPYP (pH 7.0). The difference from the former is explained by the pH dependence (manuscript in preparation). On the other hand, the far-UV CD peak of M100L shifted from 222 to 223 nm by light unlike that of the wild type. Therefore, it appears that the secondary structure of M100L$_M$ is significantly different from the wild type.

Large absorbance changes that suggest global conformational change were observed in the amide mode region of the difference FTIR spectra for truncated PYPs (Figures 3 and 4). However, absorbance changes attributable to the structural change of the β-sheet for truncated PYPs were smaller than that for iPYP, suggesting that the structural

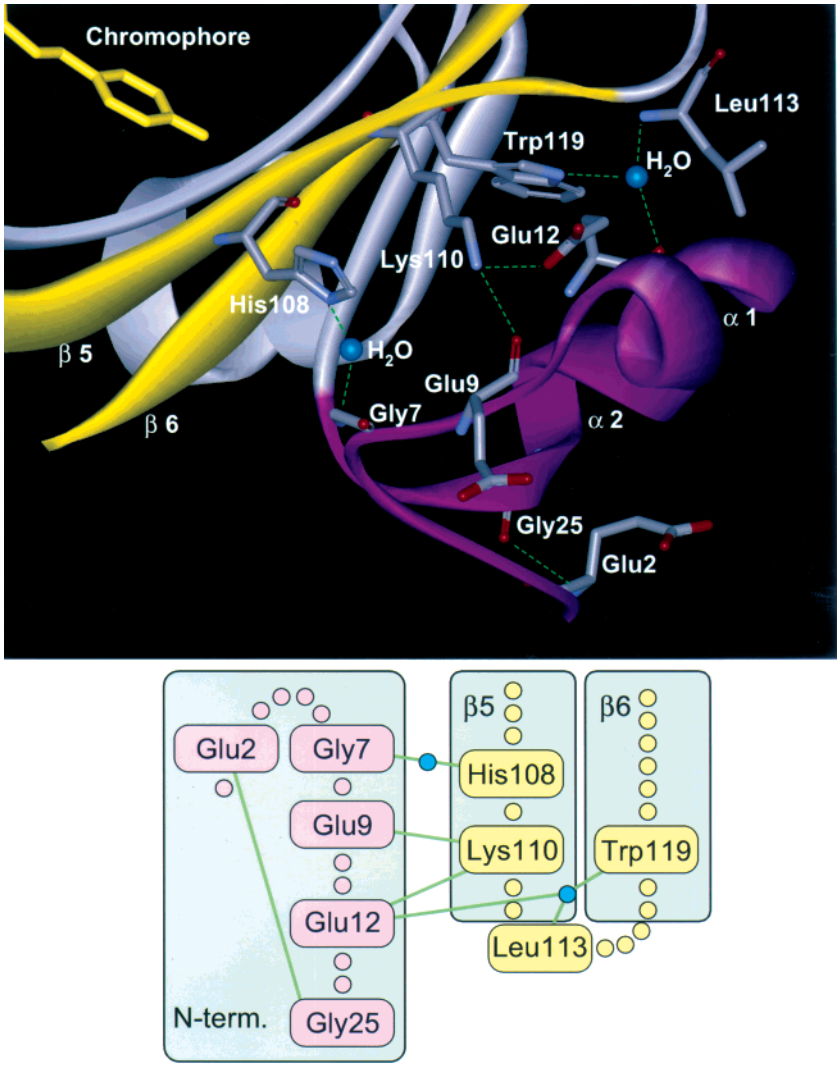

FIGURE 6: Electrostatic interaction between the N-terminal cap and the β-scaffold derived from the crystal structure (PDB code 2PHY). Water molecules are represented in blue. The salt linkage and hydrogen bonds (green) are present between the N-terminal cap (pink) and β5-β6 (yellow).

change of the β-sheet is closely correlated with the N-terminal loop.

The present experiment, along with our previous work (*23*, *24*), narrows down the possible amino acid residues responsible for the conformational change of PYP. Truncation of positions 1−6 (T6) results in a marked difference in amide I modes of the FTIR spectra (Figure 4) and ~100-fold longer lifetime of the M intermediate (Figure 5). Additional truncation of positions 7−15 results in a rather smaller shift in amide I modes and ~15-fold longer lifetime than $T6_M$. Truncation of positions 16−23 has little effect on FTIR spectra and ~4-fold longer lifetime than $T15_M$. The increase of R_g upon the formation of PYP_M is 1.1 Å for T6 and 0.7 Å for T15 and T23 (*23*). These observations indicate that positions 1−15 are important for the conformational change that causes the absorbance change of the amide mode and dimensional increase.

The most prominent amide I mode at 1625 cm^{-1} for $iPYP_M$ (Figure 4) has been assigned to the antiparallel β-structure mode (*18*). Thus, its complementary bands at 1635 and 1646 cm^{-1} could be assigned to the antiparallel β-structure mode. Note that these difference FTIR spectra do not indicate the unfolding of the β-sheet because the pair to β-structure mode of the dark state was observed for the M intermediate. As the 1646 cm^{-1} band shifted to 1635 cm^{-1} in truncated PYPs, the β-strand(s) for this mode are likely to interact with the N-terminal region. There is no β-sheet structure in the N-terminal region, but positions 1−15 are located close to the β-scaffold segment (β4-β6), suggesting that the structural change of the β-scaffold accounts for the change in the amide mode of the FTIR spectra. FTIR and CD spectroscopies also demonstrated structural disorder of the α-helices, even for T23, which lacks α1 and α2, indicating the disorder of α3, α4, and/or α5. In fact, a molecular dynamics simulation predicted structural changes around Thr50 in α3 and Met100 between β4 and β5 (*37*).

The difference absorbance at 1625 cm^{-1} accounts for one to two amide bond(s). However, the quantitative analysis using the difference spectra would not make sense because it is likely that the amide bands of the dark state and M intermediates are significantly overlapping.

The decay of PYP_M was affected by salt concentration. We have reported that the effect of the inorganic ion on the decay of PYP_M depends on the ionic strength, whereas that of the organic ion such as citrate has the specificity (*13*). It suggests that the mechanism of stabilization of PYP_M by the

inorganic ion is different from that of the organic ion. The most plausible acceptor of citrate is Arg52, located near the chromophore. However, because the effect of NaCl is different from citrate, NaCl does not necessarily affect the electrostatic interaction near the chromophore.

The dependency of the decay rate constant of *i*PYP_M on the NaCl concentration was qualitatively similar to $T6_M$: NaCl decelerates the decay of M intermediates up to 2−3 times at <500 mM but accelerates it at >1 M. However, for $T15_M$ and $T23_M$, NaCl accelerated their decays at >100 mM but never decelerated decay. In general, electrostatic interactions, such as hydrogen bonds or salt linkages, are weakened by salt. The Debye lengths at 100 and 1000 mM NaCl were calculated to be 10 and 3 Å, respectively. Because they are comparable to the hydrogen-bond length, it is reasonable to speculate that the effect of NaCl is the shielding of the polar residue(s) and/or the charged residue(s). Therefore, for *i*PYP and T6 at low salt concentrations, the electrostatic interaction accelerates the recovery of the dark states by 2−3 times. It is weakened by salt at 100−500 mM, resulting in salt-dependent stabilization of PYP_M. As this interaction is lost by truncating Met1-Leu15, the amino acid residues in this region would be involved in this interaction. However, the NaCl dependent acceleration of decay of PYP_M at high concentration was observed in all PYPs. At high salt concentration, the hydration shell of the protein surface is broken, and the water molecule in the protein is pulled out. As a result, electrostatic attractions that have been disturbed by water grow stronger, resulting in a fast recovery of PYP. Alternatively, electrostatic repulsion is weakened by salt at high concentrations, and the hydrophobic interaction grows relatively strong. Since this phase was seen in all samples, amino acid residues in the main part of PYP should be responsible for this reaction.

The observations described previously suggest that the recovery of PYP from PYP_M is partially promoted by electrostatic interactions between positions 1−15 and the β-scaffold. Electrostatic interactions between the N-terminal cap and the β-scaffold derived from the crystal structure (*38*) are shown in Figure 6. The N-terminal loop lies in parallel to the plane of the β-sheet. A salt linkage is present between the side chains of Glu12 and Lys110. The amide oxygen of Glu9 is directly hydrogen bonded to the amino group of Lys110. A water molecule mediates the hydrogen bond between the amide nitrogen of Gly7 and the imidazole nitrogen of His108. The amide oxygen of Glu12, amide nitrogen of Leu113, and indole nitrogen of Trp119 are hydrogen bonded by sharing a single water molecule. These interactions are localized to the region conserved in T6 but lost in T15 (Gly7-Leu15). These differences are consistent with the significant difference in nature between T6 and T15. The truncation of Met1-Phe6 has the greatest effect on the lifetime of PYP_M and the amide mode of the difference FTIR spectra. Unexpectedly, the direct electrostatic interaction between Met1-Phe6 and β-scaffold was not found in the crystal structure. Instead, the amide nitrogen of Glu2 and amide oxygen of Gly25 is hydrogen bonded to form the N-terminal loop. Lack of this hydrogen bond would cause a disorder of the N-terminal loop, which would weaken the interactions between Gly7-Glu12 and β5-β6.

The side chains of Glu12, His108, Lys110, and Trp119 are involved in the interactions between the N-terminal cap and the β-scaffold. These residues are conserved in *Ectothiorhodospira halophila*, *Rhodothalassium salexigens* (*39*), *Rhodobacter sphaeroides* (*40*), *Rhodobacter capsulatus* (*41*), and *Halochromatium salexigens* (*42*), except for Glu12. However, as Asp is substituted into position 12 of *R. sphaeroides* and *R. capsulatus*, the electrostatic property of this position is conserved. These high conservations suggest that interaction between the N-terminal cap and the β-scaffold promotes the structural changes of PYP_M.

Our previous SAXS experiments suggested that the N-terminal loop is detached from the main part on the formation of PYP_M (*23*). In this model, the interactions between Gly7-Glu12 and β5-β6 are broken in PYP_M. Thus, conversion from PYP_M to PYP involves the reformation of these interactions. However, chromophore bands in the FTIR spectra including cis/trans markers (1286/1301 cm^{-1} (*31*) and 1004/1058 cm^{-1} (*43*)) were observed in all truncated PYPs, suggesting that restoration of the dark state chromophore including cis → trans isomerization and deprotonation is not independent of restoration of the protein moiety. Namely, the N-terminal region also promotes protein structural change, as well as isomerization and/or the deprotonation of the chromophore. It seems to be curious that the rate-limiting factor is present far from the chromophore. However, the protein conformational change and chromophore change take place cooperatively. Most of the HSQC cross-peaks are lost in PYP_M (*19*), suggesting that the structure of PYP_M is in equilibrium among the multiple substates. Therefore, some substates would have interaction between Gly7-Glu12 and β5-β6 and effectively restore the chromophore to the dark state.

REFERENCES

1. Cusanovich, M. A., and Meyer, T. E. (2003) *Biochemistry 42*, 4759−4770.
2. Pellequer, J-. L., Wager-Smith, K. A., Kay, S. A., and Getzoff, E. D. (1998) *Proc. Natl. Acad. Sci. U.S.A. 95*, 5884−5890.
3. Sprenger, W. W., Hoff, W. D., Armitage, J. P., and Hellingwerf, K. J. (1993) *J. Bacteriol. 175*, 3096−3104.
4. Meyer, T. E., Yakali, E., Cusanovich, M. A., and Tollin, G. (1987) *Biochemistry 26*, 418−423.
5. Hoff, W. D., Van Stokkum, I. H. M., Van Ramesdonk, H. J., Van Brederode, M. E., Brouwer, A. M., Fitch, J. C., Meyer, T. E., Van Grondelle, R., and Hellingwerf, K. J. (1994) *Biophys. J. 67*, 1691−1705.
6. Imamoto, Y., Kataoka, M., and Tokunaga, F. (1996) *Biochemistry 35*, 14047−14053.
7. Ujj, L., Devanathan, S., Meyer, T. E., Cusanovich, M. A., Tollin, G., and Atkinson, G. H. (1998) *Biophys. J. 75*, 406−412.
8. Imamoto, Y., Kataoka, M., Tokunaga, F., Asahi, T., and Masuhara, H. (2001) *Biochemistry 40*, 6047−6052.
9. Bogomolni, R. A., and Spudich, J. L. (1982) *Proc. Natl. Acad. Sci. U.S.A. 79*, 6250−6254.
10. Hoff, W. D., Jung, K. H., and Spudich, J. L. (1997) *Annu. Rev. Biophys. Biomol. Struct. 26*, 223−258.
11. Imamoto, Y., Shichida, Y., Hirayama, J., Tomioka, H., Kamo, N., and Yoshizawa, T. (1992) *Photochem. Photobiol. 56*, 1129−1134.
12. Genick, U. K., Borgstahl, G. E., Ng, K., Ren, Z., Pradervand, C., Burke, P. M., Šrajer, V., Teng, T. Y., Schildkamp, W., McRee, D. E., Moffat, K., and Getzoff, E. D. (1997) *Science 275*, 1471−1475.
13. Shimizu, N., Kamikubo, H., Mihara, K., Imamoto, Y., and Kataoka, M. (2002) *J. Biochem. (Tokyo) 132*, 257−263.
14. Imamoto, Y., Mihara, K., Hisatomi, O., Kataoka, M., Tokunaga, F., Bojkova, N., and Yoshihara, K. (1997) *J. Biol. Chem. 272*, 12905−12908.
15. Xie, A., Hoff, W. D., Kroon, A. R., and Hellingwerf, K. J. (1996) *Biochemistry 35*, 14671−14678.

16. Van Brederode, M. E., Hoff, W. D., Van Stokkum, I. H., Groot, M. L., and Hellingwerf, K. J. (1996) *Biophys. J. 71*, 365−380.
17. Brudler, R., Rammelsberg, R., Woo, T. T., and Getzoff, E. D. (2001) *Nat. Struct. Biol. 8*, 265−270.
18. Xie, A., Kelemen, L., Hendriks, J., White, B. J., Hellingwerf, K. J., and Hoff, W. D. (2001) *Biochemistry 40*, 1510−1517.
19. Rubinstenn, G., Vuister, G. W., Mulder, F. A., Düx, P. E., Boelens, R., Hellingwerf, K. J., and Kaptein, R. (1998) *Nat. Struct. Biol. 5*, 568−570.
20. Ohishi, S., Shimizu, N., Mihara, K., Imamoto, Y., and Kataoka, M. (2001) *Biochemistry 40*, 2854−2859.
21. Lee, B. C., Croonquist, P. A., Sosnick, T. R., and Hoff, W. D. (2001) *J. Biol. Chem. 276*, 20821−20823.
22. Sasaki, J., Kumauchi, M., Hamada, N., Oka, T., and Tokunaga, F. (2002) *Biochemistry 41*, 1915−1922.
23. Imamoto, Y., Kamikubo, H., Harigai, M., Shimizu, N., and Kataoka, M. (2002) *Biochemistry 41*, 13595−13601.
24. Harigai, M, Yasuda, S., Imamoto, Y., Yoshihara, K., Tokunaga, F., and Kataoka, M. (2001) *J. Biochem. (Tokyo) 130*, 51−56.
25. van der Horst, M. A., van Stokkum, I. H., Crielaard, W., and Hellingwerf, K. J. (2001) *FEBS Lett. 497*, 26−30.
26. Mihara, K., Hisatomi, O., Imamoto, Y., Kataoka, M., and Tokunaga, F. (1997) *J. Biochem. (Tokyo) 121*, 876−880.
27. Imamoto, Y., Ito, T., Kataoka, M., and Tokunaga, F. (1995) *FEBS Lett. 374*, 157−160.
28. Chen, Y. H., Yang, J. T., and Chau, K. H. (1974) *Biochemistry 13*, 3350−3359.
29. Chin, D. H., Woody, R. W., Rohl, C. A., and Baldwin, R. L. (2002) *Proc. Natl. Acad. Sci. U.S.A. 99*, 15416−15421.
30. Andrade, M. A., Chacon, P., Merelo, J. J., and Moran, F. (1993) *Protein Eng. 6*, 383−390.
31. Imamoto, Y., Shirahige, Y., Tokunaga, F., Kinoshita, T., Yoshihara, K., and Kataoka, M. (2001) *Biochemistry 40*, 8997−9004.
32. Arrondo, J. L., Muga, A., Castresana, J., and Goñi, F. M. (1993) *Prog. Biophys. Mol. Biol. 59*, 23−56.
33. Cantor, C. R., and Schimmel, P. R. (1980) *Biophysical Chemistry: Techniques for the Study of Biological Structure and Function*, W. H. Freeman and Co., New York.
34. Chen, E., Gensch, T., Gross, A. B., Hendriks, J., Hellingwerf, K. J., and Kliger, D. S. (2003) *Biochemistry 42*, 2062−2071.
35. Woody, R. W. (1996) in *Circular Dichroism and the Conformational Analysis of Biomolecules* (Fasman, G. D., Ed.), Chapter 2, pp 25−68, Plenum Press, New York.
36. Weaver, T. M. (2000) *Protein Sci. 9*, 201−206.
37. Shiozawa, M., Yoda, M., Kamiya, N., Asakawa, N., Higo, J., Inoue, Y., and Sakurai, M. (2001) *J. Am. Chem. Soc. 123*, 7445−7446.
38. Borgstahl, G. E. O., Williams, D. R., and Getzoff, E. D. (1995) *Biochemistry 34*, 6278−6287.
39. Kort, R., Hoff, W. D., Van West, M., Kroon, A. R., Hoffer, S. M., Vlieg, K. H., Crielaard, W., Van Beeumen, J. J., and Hellingwerf, K. J. (1996) *EMBO J. 15*, 3209−3218.
40. Kort, R., Phillips-Jones, M. K., van Aalten, D. M., Haker, A., Hoffer, S. M., Hellingwerf, K. J., and Crielaard, W. (1998) *Biochim. Biophys. Acta 1385*, 1−6.
41. Jiang, Z., and Bauer, E. C. (1998) GenBank Accession Number AF064095.
42. Koh, M., Van Driessche, G., Samyn, B., Hoff, W. D., Meyer, T. E., Cusanovich, M. A., and Van Beeumen, J. J. (1996) *Biochemistry 35*, 2526−2534.
43. Unno, M., Kumauchi, M., Sasaki, J., Tokunaga, F., and Yamauchi, S. (2002) *Biochemistry 41*, 5668−5674.

BI034814E